On the Photocatalytic Performance of Indium Tantalate and its Modifications

Maoiheb Douiheche, Robert Haberkorn, and Horst P. Beck

Institute for Inorganic and Analytical Chemistry, Saarland University, Saarbrücken, Germany

Reprint requests to Prof. Dr. Horst P. Beck. Fax: +49 (0)681 302 4233.
E-mail: hp.beck@mx.uni-saarland.de

Z. Naturforsch. **2008**, *63b,* 1160 – 1168; received May 28, 2008

The photocatalytic activity of $InTaO_4$ has been studied regarding the effect of a substitution of In by Ni, of the performance of NiO as well as Ag_2O as co-catalysts, and especially of the products of different methods of preparation (solid state reaction and/or sol-gel process) and their particle sizes. Solid state reactions and sol-gel procedures were used to synthesise different products for the catalytic reaction in a reactor vessel equipped with a mercury UV lamp. The optical properties and the band gap values of the different products were evaluated by reflectance spectroscopy, and the microstructure parameters of the crystalline products were determined by an elaborate profile analysis of the X-ray diagrams. The evolution of H_2 and O_2 under irradiation was quantified by a GC setup. The causes for the deviations of the performance of these catalysts from the values reported elsewhere are discussed.

Key words: Photocatalysis, Indium Tantalate, Factors for Catalytic Efficiency, Preparation Strategies

Introduction

Photocatalytic reactions have been in the focus of many studies in the last years. However, the direct cleavage of water as the most interesting application was realised with only few systems where the size of the semiconductor band gap and its location on the potential scale fit into the needs of the oxidation and reduction steps of the complex reaction. This is why more studies have dealt with photodegradation of organic compounds where only one of the reaction steps takes place, a second one being run in a reaction with a sacrificial additive. Some model setups of solar cells are based on such strategies as well.

Because water cleavage itself is the most important process the efforts have shifted from such model experiments to a more or less systematic search for new heterogeneous catalytic systems with higher light-conversion rates. Two main strategies have been followed. A first one is the more or less systematic screening of many compounds for catalytic activity, sometimes done in a combinatorial-like approach, and a second one focuses on the improvement of the performance of known catalysts by variation of the composition, by doping and by combination with co-catalysts. Some of the reports in the literature seem rather spectacular, however, many of them lack well founded data regarding the long term stability of the catalysts and especially the reproducibility of experimental results.

Our own efforts are directed to the investigation of details of the complex reaction mechanism and of the factors influencing the performance of catalytic systems. To this end we have chosen an example which has aroused much interest. It has been shown that the catalytic power of $InTaO_4$ is quite extraordinary even when using visible light only, and that NiO applied as a co-catalyst on the surface can enhance the desired effects. Several papers have appeared describing the structure of the compound and its photocatalytic activity. A key reference is the work by Zou *et al.* [1].

In this paper we report on our investigations directed to the influence of preparation routes, structural and microscopic variations of the compounds and the instrumental setup on the efficiency of this catalyst. It appears that these details have a great influence.

Experimental Section

Preparations

Our study has comprised investigations on the catalytic light-conversion efficiency of $InTaO_4$ prepared in different forms and by different routes. As a sort of standard material we have prepared the compound *via* a conventional solid state route by repeatedly firing stoichiometric mixtures of the

0932–0776 / 08 / 1000–1160 $ 06.00 © 2008 Verlag der Zeitschrift für Naturforschung, Tübingen · http://znaturforsch.com

binary compounds In_2O_3 and Ta_2O_5 (ChemPur, Germany) at 1100 °C in platinum crucibles under normal atmosphere according to Eq. 1.

$$In_2O_3 + Ta_2O_5 \rightarrow 2\,InTaO_4 \quad (1)$$

XRD investigations showed the products to be single-phase compounds according to published data [1, 2]. In order to have specimens with different particle and crystallite sizes we have treated fractions of this material in a ball mill for 6 or for 12 h. We have then modified the procedure by adding differing amounts of NiO (Kristallhandel Kelpin, Germany) during synthesis according to Eq. 2

$$(1-x)\,In_2O_3 + Ta_2O_5 + 2x\,NiO \rightarrow 2\,In_{1-x}Ni_xTaO_{4-x/2} \quad (2)$$

in order to substitute In by Ni, and to create anion defects in the structure of $InTaO_4$.

The dopant concentration was varied only in the range $0 < x < 0.2$ because beyond this higher limit composition the appearance of $NiTa_2O_6$ was noted in the XRD diagrams. The homogeneous incorporation of the dopant could be tracked by a linear Végard-type contraction of the cell volume from 144.0 to 142.9 Å^3 in the range $0 < x < 0.15$. These findings are consistent with those reported by Zou *et al.* [1].

For studies with "NiO" as a co-catalyst we have loaded the above mentioned products with a NiO/Ni composite by impregnating them with an aqueous solution containing 100 ppm of $Ni(NO_3)_2 \cdot 6\,H_2O$ (Fluka, Switzerland) for 1 h and drying them after filtering at 350 °C for 1 h. The samples were then exposed at 500 °C to a 7 vol.-% H_2/Ar_2 gas stream and finally partly re-oxidised at 200 °C in air. (Such samples are named NiO_y/Ni *x* %-$InTaO_4$ in the text and in the Tables according to the content *x* of the dopant Ni.) It has been assumed [1] that a double layer-structure of Ni and NiO (termed NiO_y in this text) may suppress the recombination of H_2 and O_2 which would otherwise be triggered by Ni alone. A similar series of products was produced by impregnating samples with a solution of $AgNO_3$ and drying at 350 °C to give Ag_2O_z/$InTaO_4$ composites. In this case further steps were omitted.

A second set of compounds was synthesised in a sol-gel adapted process, to our knowledge used for the first time for the preparation of $InTaO_4$. To obtain 1 g of $InTaO_4$ an amount of 0.979 g indium(III) acetylacetonate (2.78 mmol) (ABCR, Germany) was dissolved in 100 mL of absolute ethanol yielding a dark brown suspension which cleared up after adding some drops of glacial acetic acid and adjusting the pH to about 9 – 10 with absolute ethylenediamine. An equimolar amount of tantalum ethoxide dissolved in 100 mL of absolute ethanol was added dropwise with stirring, and stirring was continued for 2 h before slowly adding 20 mL of dist. water. The soft gel formed was washed several times with water, separated again by centrifugation and dried at

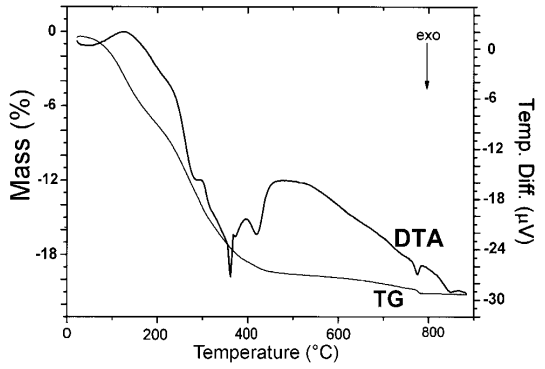

Fig. 1. TG/DTA plot of an $InTaO_4$ precursor gel dried at 40 °C.

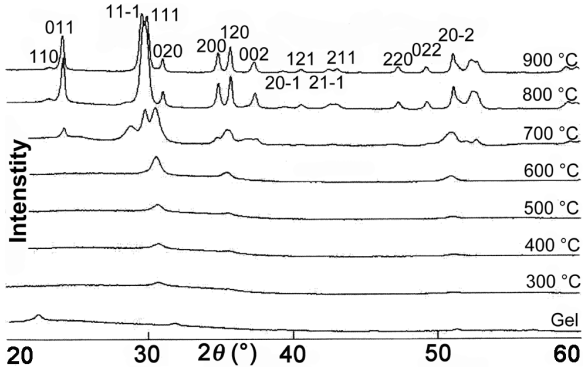

Fig. 2. X-Ray diagrams of intermediates and endproducts of the sol-gel route.

40 °C in a rotary evaporator to yield a fine light-brown powder.

Fig. 1 shows the results of a TG-DTA scan (Netzsch STA 409, Germany) of the dried gel up to 850 °C. Weight loss begins immediately at about 50 – 60 °C accompanied by a slight endothermic effect due to the evaporation of humidity. A strong decrease in weight from about 100 up to 430 °C is accompanied by strongly exothermic reactions with occasional caloric outbursts. Up to about 770 °C the weight then decreases only very slowly. The small step at 780 °C accompanied by a distinct exothermic effect is evidently due to a crystallisation procedure. To elucidate the process in more detail we have carried out a calcination procedure in several 100 °C steps from 300 to 900 °C.

X-Ray diagrams of the intermediates and the end product were taken with a D5000 diffractometer (Siemens, Germany) in Bragg-Brentano geometry using a position-sensitive detector and Cu$K_{\alpha 1}$ radiation, or with a Guinier-type system with an imaging plate detector (Huber, Rimsting, Germany). A selection of diagrams taken with the latter system is displayed in Fig. 2. Very weak reflections from the primary gel show the existence of some scarcely crystalline $In(OH)_3$.

Table 1. Rates of gas evolution and crystallographic parameters of the photocatalysts. (ssr: prepared by solid state reaction; sg: sol-gel preparation; x hg: milled for x h).

	Lattice parameters				Microstructure parameters and wavelength			Rate of evolution (μmol h^{-1})	
Photocatalyst	*a*	*b*	*c*	β	D_{vol}	ε_0	E_g	H_2	O_2
$InTaO_4$-ssr	5.1583(1)	5.7765(1)	4.8321(1)	91.42(1)	139(1)	0.087(1)	3.30	5.656	1.213
$InTaO_4$-sg (900 °C)	5.1417(1)	5.7560(1)	4.8110(1)	90,95(1)	47.5(3)	0.164(3)	2.99	1.353	0.460
$InTaO_4$-6hg	5.1610(25)	5.7804(29)	4.8310(27)	91.28(1)	41(1)	0.177(3)	3.26	6.254	0.419
$InTaO_4$-12hg	5.1619(48)	5.7810(46)	4.8302(63)	91.14(5)	41(1)	0.245(11)	3.76	5.685	0.934
Ni 5 %-$InTaO_4$-ssr	5.1569(1)	5.7758(1)	4.8251(1)	91.36(1)	223(4)	0.102(1)	3.12	3.526	1.083
Ni 10 %-$InTaO_4$-ssr	5.1535(1)	5.7712(1)	4.8203(1)	91.35(1)	361(27)	0.112(1)	3.11	2.791	1.234
Ni 15 %-$InTaO_4$-ssr	5.1508(1)	5.7651(1)	4.8130(1)	91.32(1)	193(3)	0.125(1)	3.20	1.439	0.719
NiO_y /$InTaO_4$-ssr	–	–	–	–	–	–	–	0.119	0.076
NiO_y/Ni 5 %-$InTaO_4$-ssr	–	–	–	–	–	–	–	0.557	0.152
NiO_y/Ni 10 %-$InTaO_4$-ssr	–	–	–	–	–	–	–	0.468	0
Ag_2O_z/$InTaO_4$-ssr	–	–	–	–	–	–	–	3.844	0.216
Ag_2O_z/Ni 5 %-$InTaO_4$-ssr	–	–	–	–	–	–	–	3.279	0.156
Ag_2O_z/Ni 10 %-$InTaO_4$-ssr	–	–	–	–	–	–	–	3.105	0

From 300 °C to about 700 °C broad reflections of In_2O_3 can be discerned which disappear at 800 °C. Evidently the hydrolysis of the two starting compounds proceeds at quite different rates, and In tends to be segregated at least partially in the form of a binary hydroxide or oxide which crystallises fairly well even at low temperatures. There is no indication of a Ta-containing crystalline compound or any In-Ta intermediates in the X-ray diagrams taken after treatment at lower temperatures.

The diagrams taken after heating to 800 and 900 °C show an interesting phenomenon. First they prove that $InTaO_4$ – which is usually synthesised by annealing the mixture of the binaries for a long time at temperatures of 1100 °C or above – is already formed at quite low temperatures by this "sol-gel route". Secondly, the $InTaO_4$ part of the sol-gel product is at first formed in a PbO_2-type structure where In and Ta are distributed randomly on the cation positions. This form is otherwise to be expected as a high-temperature modification which has been shown to be formed well above 1500 °C [2]. The sol-gel approach yields this form at lower temperatures according to the Ostwald rule. The diagram taken after the 900 °C treatment then shows the orthorhombic → monoclinic symmetry reduction by ordering of the cations in the wolframite-type arrangement in the splitting of reflections.

Characterisation of materials

The efficiency of a photocatalytic system depends on many factors of which the positions of the Fermi level and the conduction band are only two important components. The fate of the $h^{\bullet}/e^{-}$ pairs, their lifetime, migration velocity, and the possibility of trapping these species are also important aspects of the complex process.

In order to correlate intrinsic properties of the different materials with their catalytic performance we have investigated their electronic properties by UV/Vis reflectance spectroscopy and their microstructure (crystallite size and strain) by an elaborate profile analysis of X-ray powder diagrams in the hope to correlate the catalytic power with the internal defect structure.

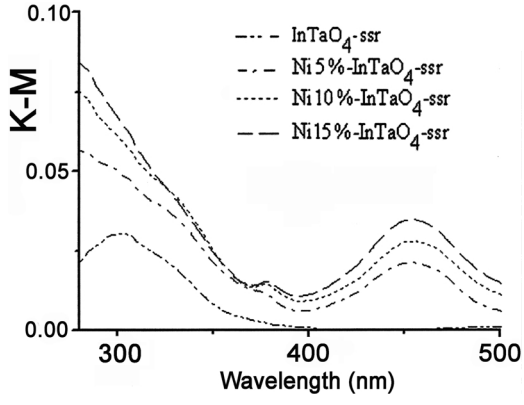

Fig. 3. Kubelka-Munk functions according to reflectance spectra of pure and doped $InTaO_4$ prepared by solid-state reaction.

Reflectance spectra were recorded with a UV/Vis NIR spectrometer Lambda 19 (Perkin Elmer) mainly in the range between 200 and 500 nm. 0.1 g of finely ground specimens were diluted with 0.2 g of MgO for the measurements, and the reflectivity was compared with that of pure MgO. The size of the band gap was estimated by extrapolating the slope of the Kubelka-Munk function derived from these spectra to a boundary wave length λ_b according to E_g [eV] = 1240/λ_b (see Fig. 3). The band gap seems to increase upon prolonged milling of $InTaO_4$ prepared by solid-state reactions from 3.30 to 3.76 eV. On the other hand it slightly decreases upon doping the material with 5 – 10 % Ni to 3.12 eV and then increases again to 3.70 eV for 15 % Ni in $InTaO_4$ (see also Table 1). The most pronounced effect is observed in the sol-gel

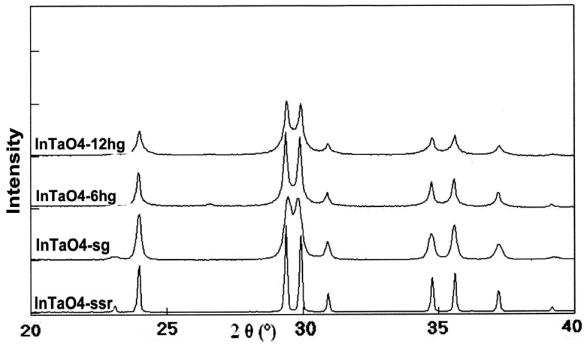

Fig. 4. X-Ray diagrams of differently treated products (see text).

product with a band gap of 2.99 eV. However, these measurements alone give no information about the absolute position of the bands on the red-ox scale.

The crystallographic and microstructure parameters were determined using the programmes TOPAS [3] and FORMFIT [4, 5] where the effects of apparatus parameters, size and microstrain can be taken into account giving the mean column height L_{vol} and the microstrain ε_0. Data are compiled in Table 1.

As an example, parts of the X-ray diagrams of differently treated $InTaO_4$ are compared in Fig. 4. The broadening of reflections on milling is clearly seen in the sequence $InTaO_4$-ssr, -6hg, -12hg (for the nomenclature used see Table 1). Least-squares refinement has shown a slight increase of the lattice parameters in the milled product, the angle β moving closer to 90°, which may be an indication of increasing cation disorder since the metric situation approaches that of a PbO_2-type structure mentioned above. The line width of the sol-gel product $InTaO_4$-sg is quite large so that close reflections almost coalesce. However, when looking closer it becomes obvious that the Gaussian and the Lorentzian contributions to the peak shape differ. The lattice parameters of $InTaO_4$-sg are clearly smaller than those of the solid state product (ssr), and β is even closer to 90°. However, on firing this product at higher temperatures the monoclinic angle slowly increases to the value of the ssr material. It may be conjectured that the ordering process mentioned above is incomplete, and that this is the reason for the difference in profile structure. There are distinct differences in the microstructure of $InTaO_4$-sg and $InTaO_4$-*x*hg. All relevant parameters of the different materials are compiled in Table 1.

Catalysis

The experimental setup for the photocatalytic studies is depicted in Fig. 5. Finely ground powders (300 mg) were suspended in 150 mL of distilled water by continuous stirring in an annular photoreactor (type UV-RS-1, Heraeus, Germany) where water is gently pressed through a by-pass, leaves at the bottom of the upright pyrex reactor vessel and re-enters it again at the top. A 150 W medium-pressure mercury UV lamp (type TQ150) in a water cooled quartz jacket was immersed in the centre of the vessel. In this setup many quite intense emissions in the region below 290 nm could also be used besides the typical lines at 312, 333, 360, 404, and

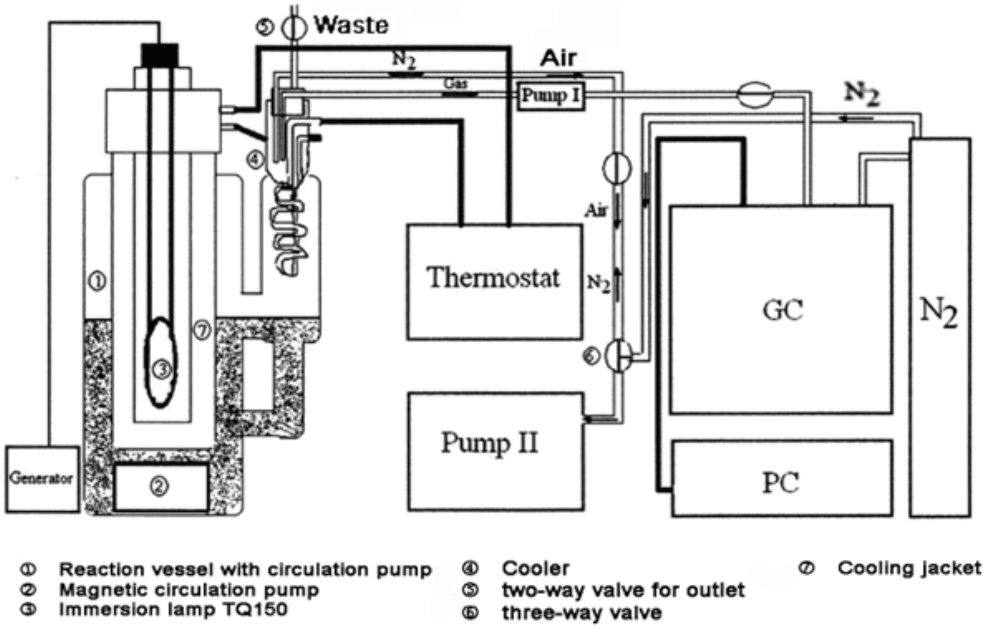

Fig. 5. Schematic view of the experimental setup for the irradiation experiments.

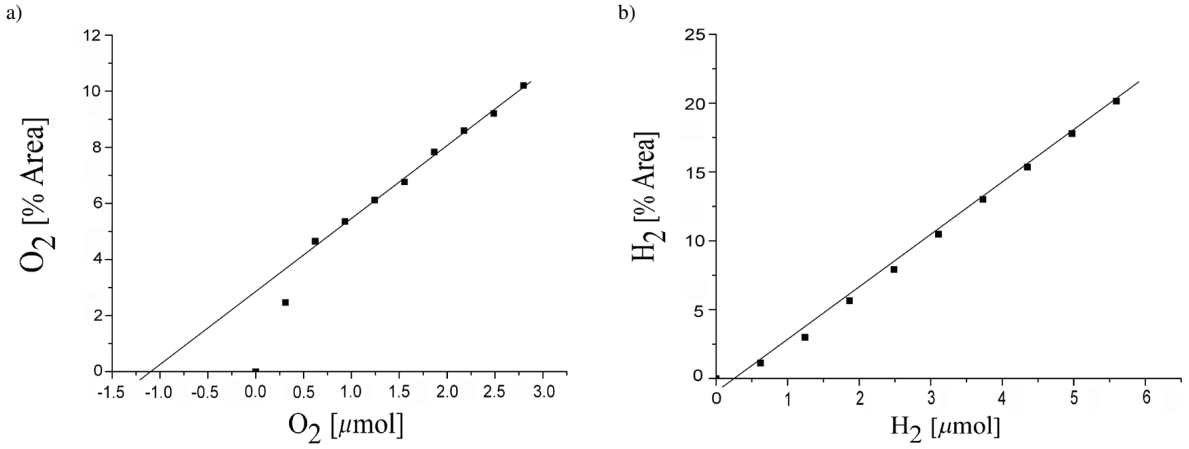

Fig. 6. Calibration curves for a) oxygen and b) hydrogen for the quantification by GC.

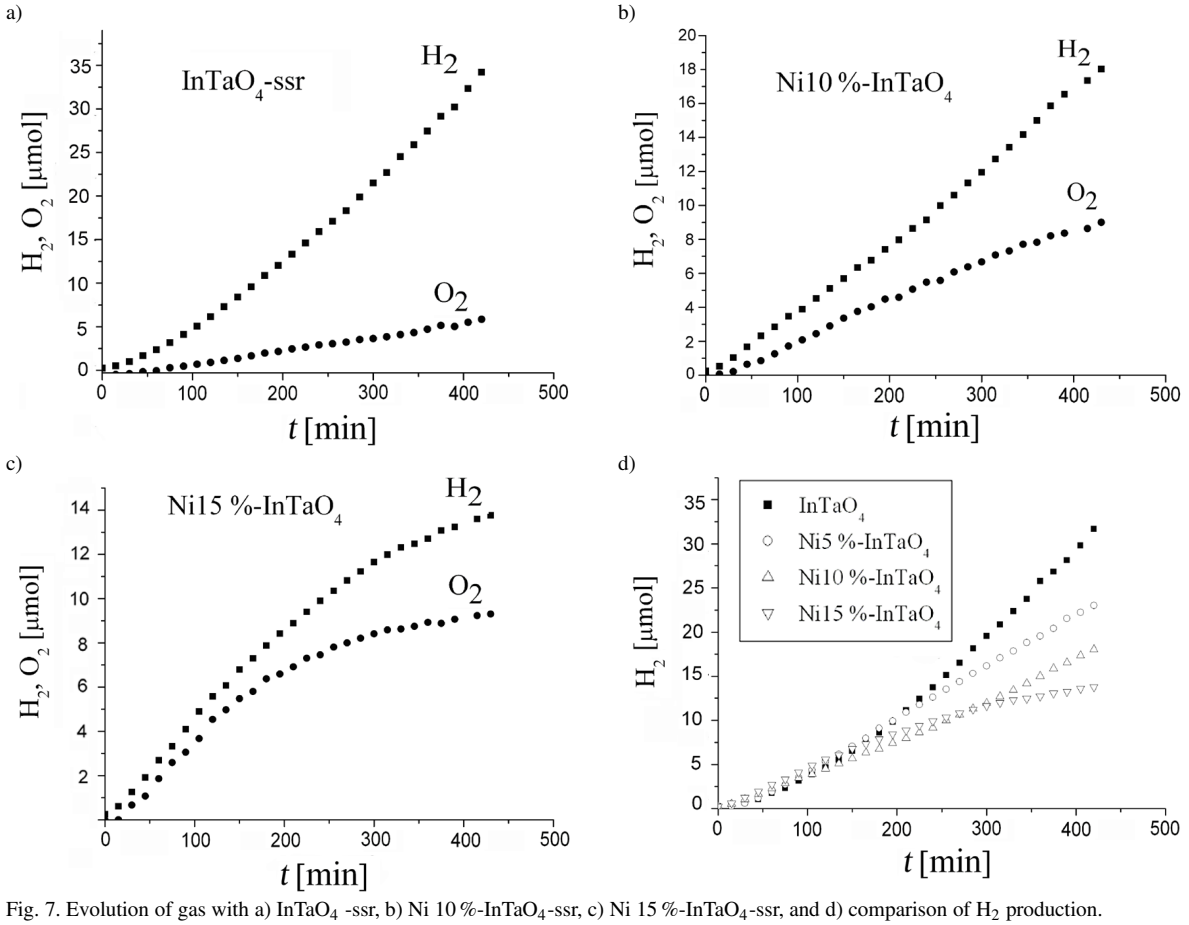

Fig. 7. Evolution of gas with a) $InTaO_4$ -ssr, b) Ni 10 %-$InTaO_4$-ssr, c) Ni 15 %-$InTaO_4$-ssr, and d) comparison of H_2 production.

435 nm. The upper compartment above the liquid phase was connected to gas tubings by means of glass fittings. The system could be evacuated and filled with nitrogen. The atmosphere was then continuously circulated with a peristaltic pump. Small volumes were extracted *via* an injection valve and analysed with an Agilent 6890 GC using a Molsieve

19095p-MS6 column (Agilent), N_2 carrier gas and a TLC detector (injector temperature 200 °C; detector temperature 250 °C; capillary length 30 m, equilibrated at 50 °C). The calibration of the entire system was done by producing a known amount of a H_2/O_2 gas mixture in the reactor by electrolysis with small Pt electrodes and using Faraday's laws. Figs. 6a and b give an example for such calibration curves. (It may be noted that there is an offset of the calibration line in the case of O_2 due to the noticeable solubility of this gas in water which has to be taken into account by the typical evaluation as used in standard addition methods in analysis.)

Results

Figs. 7a, b and c show typical results with $InTaO_4$-ssr and with material doped with 10 % and 15 % Ni. It will be noted that the H_2/O_2 relation is only fairly close to 2 : 1. The first diagram shows a sort of an activation process, whereas the latter two have a typical form showing saturation or deactivation processes. However, X-ray diagrams taken before and after prolonged catalytic activity show no change of the structure and microstructure. The example 10 % Ni-$InTaO_4$ demonstrates the long-time stability in experiments where the UV lamp was shut off and the atmosphere was renewed several times (Fig. 8).

For a better comparison, the efficiency of the compounds of this series is demonstrated by showing the H_2 evolution during 7 h in Fig. 7d. Doping with Ni reduces the activity after a certain time, for the undoped material the activity even seems to improve with time.

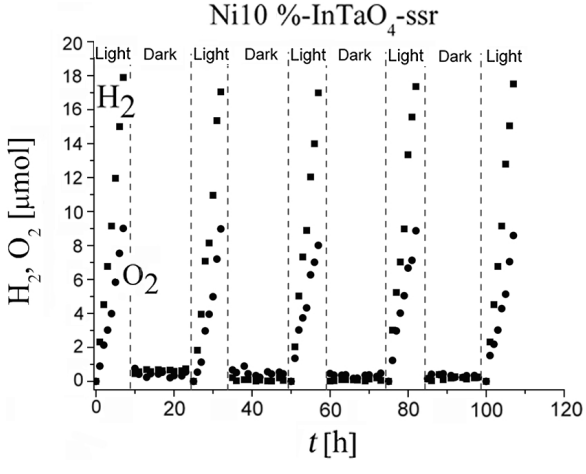

Fig. 8. Repeated photocatalytic water cleavage by Ni 10 %-$InTaO_4$-ssr.

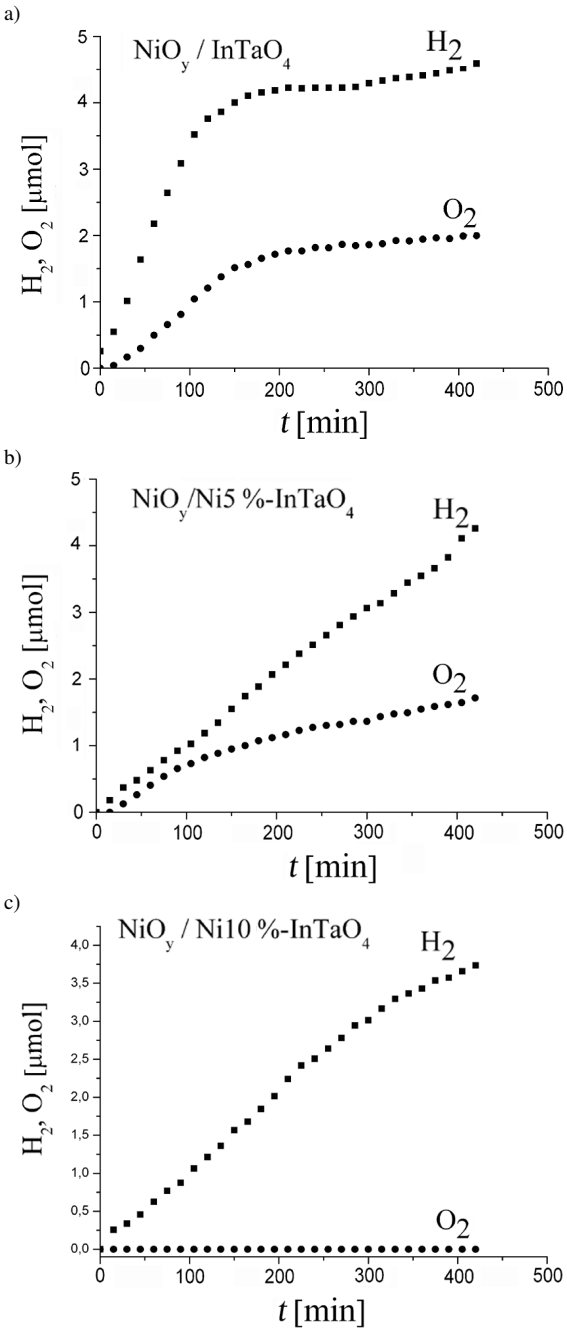

Fig. 9. Effect of NiO as co-catalyst with a) $NiO_y/InTaO_4$-ssr, b) NiO_y/Ni 5 %-$InTaO_4$-ssr, and c) NiO_y/Ni 10 %-$InTaO_4$-ssr.

The auxiliary effect of co-catalysts has been emphasised in the literature [1, 6]. Our own experience is quite different. In our experiments loading with NiO_y always reduced the activity. The great differences seen

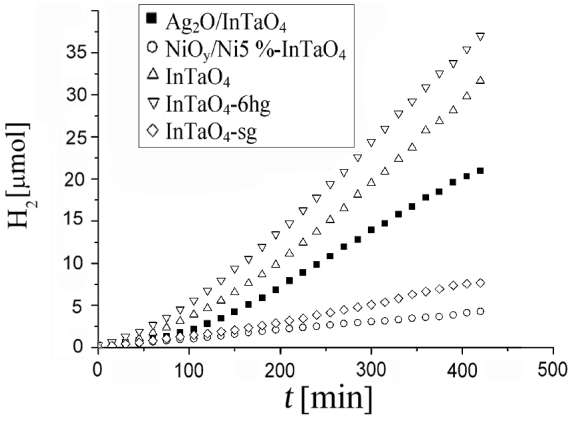

Fig. 10. Comparison of the H_2 evolution of the best products in all the compound series examined.

with material supposedly prepared by identical routes become evident when comparing Figs. 9 a, b and c. In the first case, $NiO_y/InTaO_4$ loses its activity after about 3 h. The material doped with 5 % Ni seems to be stable in the presence of this co-catalyst, but it is not very efficient, and in the case of NiO_y/Ni 10 %-$InTaO_4$ there is virtually no evolution of oxygen. (Thus, allegedly "similar" materials behave quite differently. Similar "discontinuities" with rising Ni content are found in reports of Zou [1] who was one of the first to study these materials.) In this last mentioned case there is evidently a change in the mechanism of the oxidation step leading to the formation of other species such as H_2O_2 instead of O_2. These could indeed be detected by the titanyl peroxide reaction. The powders of the series with Ag_2O as co-catalyst behave differently. In this case, the coating does not suppress the activity very much, and the additional doping with Ni leads to about the same reduction of the activity as in the $InTaO_4$-ssr series. However, in all these cases the development of O_2 is completely suppressed.

Finally, Fig. 10 gives a comparison of the milled and the sol-gel products together with the best examples of all the other compound series. Compared with untreated $InTaO_4$-ssr, short milling ($InTaO_4$-6hg) enhances the photocatalytic yield, but prolonged milling ($InTaO_4$-12hg) reduces it again. This behaviour can be understood as an effect caused by the smaller size of the particles after milling and their larger surface, and it may also be correlated with the microstructure parameters of the crystallites (see Table 1). The ε_0 value describing internal strain and lattice misfits is increased on milling. A certain amount of lattice defects may also improve the mobility of charge carriers and/or prevent their recombination. REM pictures (Fig. 11) and X-ray reflection profile analyses show that longer mechanical treatment does not give much smaller particles or crystallites but evidently generates either too high defect concentrations or local amorphisation which will then offer traps or recombination centres for the charge carriers. This is seen in the parameters determined for the internal strain of the crystallites. A similar explanation may be given for the very poor catalytic performance of the sol-gel product $InTaO_4$-sg. However, as discussed above, the microstructure of this product evidently differs as seen in the form of the X-ray reflections.

Fig. 11d shows that the sol-gel product has a high inner porosity. This does not necessarily contribute to higher surface areas. It seems that the gas produced within and at the surface of the particles is rather held back by capillary effects thereby preventing further gas exchange.

The internal structure, the ordering process of the cations and probably also the surface and grain-boundary structure of the particles resulting from the different preparations are evidently quite different, and this has great influence on the different steps of the complex photocatalytic mechanism. Other than in many other cases, the preparation route *via* sol-gel reaction, which is nowadays cherished as a most promising approach to all problems, is a bad alternative to improve the photocatalytic activity of $InTaO_4$.

Conclusion

It was the aim of this work to study the influence of different preparative routes, dopant concentrations, co-catalysts, and aftertreatments on the photoactivity of $InTaO_4$, a material which has been described to be a very good catalyst for light-induced water cleavage, and we have in general tried to reproduce published data. It is not surprising that results published previously were not wholly reproduced due to the subtle differences in the preparation procedures which unknowingly always exist. On comparing our results with those published by Zou *et al.* [1] we must realise that the performance values given there are difficult to reproduce with our setup. A number of causes may be the reason for the discrepancies. First the design of the irradiation apparatus is different, and other light sources

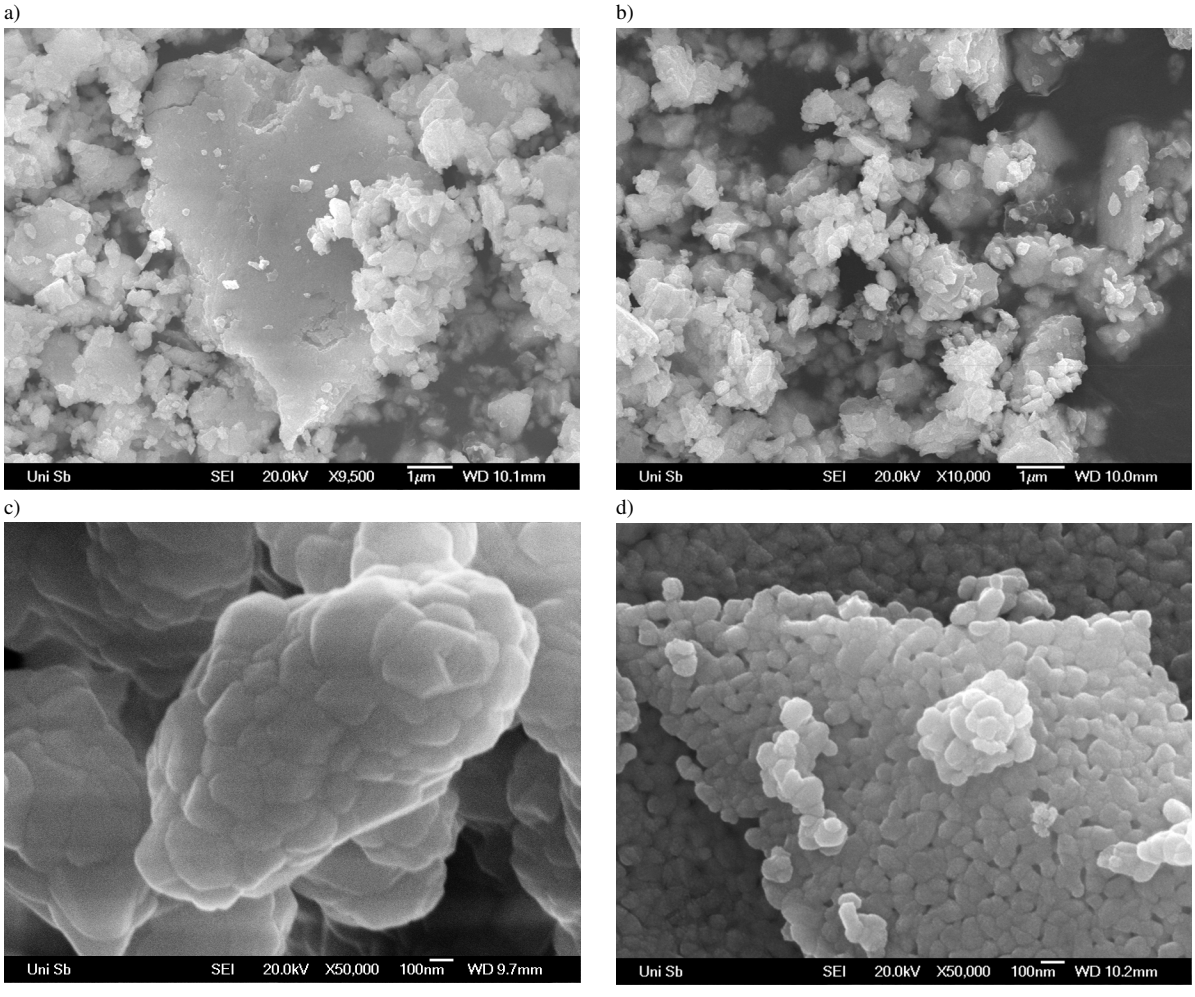

Fig. 11. REM pictures of a) $InTaO_4$-ssr, b) $InTaO_4$-6hg, c) $InTaO_4$-ssr, d) $InTaO_4$-sg, [a) and b) in low and c) and d) in high magnification].

and long-pass cut-off filters were used giving other, more continuous wavelength distributions, evidently in order to better approach the wavelengths of sunlight. Their long-pass filter is said to have a cut-off at 420 nm where maximum light energy would be 2.95 eV. Indeed they emphasize that this catalyst is especially efficient in the range of visible light. Our UV lamp has intense emissions well above this energy allowing high-energy absorptions over the band gap but only of a few spectral lines in the lower energy range (see above). This may open up quite a different light-harvesting mechanism in our case as compared with the experiments reported in the literature. The reflectance spectra of the photocatalysts show a second absorption maximum at 460 nm (Fig. 3) where the lamp used in this study has virtually no intensity. This wavelength corresponds to about 2.6 eV. Indeed, band gap values discussed in the literature are as low as this value [1]. Other authors may have seen the effect of this secondary absorption phenomenon in their photocatalytic studies.

Nevertheless, even though the activities observed in our study are much lower, qualitative differences among our different preparations give interesting insights. It becomes evident that the preparation procedure and aftertreatments play an important role. Our solid state reaction procedures closely mimic those of Zou *et al*. [1]. The large differences in catalytic power and the converse results of doping and co-catalysts may partly be interpreted as a result of the differences in apparatus setup, and here especially of the irradia-

tion conditions, but they also indicate that reproducibility to all details of the structure and microstructure is hardly achievable. The effect of preparatory conditions on the subtle differences in the microstructure of solids, decisive for their catalytic performance, is sometimes forgotten. To remind this fact is a main purpose of our paper.

Acknowledgements

We greatly appreciate the co-operation with Dr. Seiler at the Institute for Technical Chemistry, Saarland University. Financial support for one of us, Dr. M. Douiheche, has been given by the Deutsche Forschungsgemeinschaft in the frame of the Graduiertenkolleg "Hochleistungs-Werkstoffe zur effizienten Nutzung von Energieresourcen".

[1] Z. Zou, J. Ye, K. Sayama, H. Arakawa, *Nature* **2001**, *414*, 625, and refs. therein.

[2] O. Harneit, H. Müller-Buschbaum, *J. Alloys Compd.* **1993**, *194*, 101.

[3] TOPAS (version 2.1), General Profile and Structure Analysis Software for Powder Diffraction Data, Bruker AXS, Karlsruhe (Germany) **2003**.

[4] R. Haberkorn, FORMFIT (version 5.4), A Program for Determination of Microstructure from X-ray Diffraction Scans, Dudweiler (Germany) **2005**.

[5] C. E. Krill, R. Haberkorn, R. Birringer, in *Handbook of Nanostructured Materials and Nanotechnology*, Vol. 2, (Ed.: H. S. Nalwa), Academic Press, San Diego, **2000**, p. 155.

[6] Z. Zou, J. Ye, H. Arakawa, *Chem. Phys. Lett.* **2000**, *332*, 271.